



## Identifying the molecular and cellular signature of cardiac dilation following myocardial infarction<sup>☆</sup>



Merry L. Lindsey<sup>a,b,c</sup>, Yonggang Ma<sup>a</sup>, Elizabeth R. Flynn<sup>a</sup>, Michael D. Winniford<sup>a,c</sup>,  
Michael E. Hall<sup>a,c</sup>, Kristine Y. DeLeon-Pennell<sup>d,e,\*</sup>

<sup>a</sup> Mississippi Center for Heart Research, Department of Physiology and Biophysics, University of Mississippi Medical Center, 2500 N State St, Jackson, MS 39216, USA

<sup>b</sup> Research Service, G.V. (Sonny) Montgomery Veterans Affairs Medical Center, 1500 E Woodrow Wilson Ave, Jackson, MS 39216, USA

<sup>c</sup> Division of Cardiology, University of Mississippi Medical Center, 2500 N State St, Jackson, MS 39216, USA

<sup>d</sup> Research Service, Ralph H. Johnson Veterans Affairs Medical Center, 109 Bee St, Charleston, SC 29401, USA

<sup>e</sup> Division of Cardiology, Medical University of South Carolina, 30 Courtenay Dr, Charleston, SC 29425, USA

### ARTICLE INFO

#### Keywords:

Big data  
Cardiovascular disease  
Myocardial infarction  
LV dilation  
Inflammation  
Macrophage  
Proteomics

### ABSTRACT

Establishing molecular and cellular indicators that reflect the extent of dilation of the left ventricle (LV) after myocardial infarction (MI) may improve diagnostic and prognostic capabilities. We queried the Mouse Heart Attack Research Tool (mHART) 1.0 for day 7 post-MI mice (age 3–9 months, untreated males and females) with serial echocardiographic data at days 0, 1, and 7 (n = 51). Mice were classified into two subgroups determined by a median fold change of 1.6 in end-diastolic dimensions (EDD) normalized to pre-MI values; n = 26 fell below (moderate; mean of  $1.42 \pm 0.01$ ) and n = 25 fell above this cut-off (extreme; mean of  $1.79 \pm 0.01$ ;  $p < 0.001$  vs. moderate). Plasma proteomic profiling of 34 analytes measured at day 7 post-MI from male mice (n = 12 moderate and 12 extreme) were evaluated as the test dataset, and receiver operating curve (ROC) analysis was used to assess strength of biomarkers. Females (n = 6 moderate and 9 extreme) were used as the validation dataset. Both by *t*-test and characteristic (ROC) curve analysis, lower macrophage inflammatory protein-1 gamma (MIP-1 $\gamma$ ), lymphotactin, and granulocyte chemotactic protein-2 (GCP-2) were identified as plasma indicators for dilation status ( $p < 0.05$  for all). Macrophage numbers were decreased and complement C5, laminin 1, and Ccr8 gene levels were significantly higher in the LV infarcts of the extreme dilation group ( $p < 0.05$  for all). A composite panel including plasma MIP-1 $\gamma$ , lymphotactin, and GCP-2, and LV infarct Ccr8 and macrophage numbers strongly mirrored LV dilation status (AUC = 0.92;  $p < 0.0001$ ). Using the mHART 1.0 database, we determined that a failure to mount sufficient macrophage-mediated inflammation was indicative of exacerbated LV dilation.

### 1. Introduction

The cardiac wound healing process after myocardial infarction (MI) is divided into three distinct, but temporally overlapping, phases of infarct healing: an inflammatory phase, a proliferative phase, and a maturation phase [1]. Optimal healing of the left ventricle (LV) requires mechanisms to initiate an inflammatory response, mechanisms to resolve inflammation by inhibiting pro-inflammatory cytokines and clearing inflammatory cells, and mechanisms to induce repair [2–6].

Markers of inflammation, including myeloperoxidase (MPO) and white blood cell count (WBC), are strong predictors of post-MI adverse remodeling [7–9]. When WBC was used as a marker for post-MI in-hospital mortality, the pattern followed a J curve shape [10]. Patients

with  $< 1.0 \times 10^3$  cell/mL WBC had a mortality rate of 29%, which decreased to 4% in patients with  $5\text{--}6 \times 10^3$ /mL WBC. When WBC increased to over  $25 \times 10^3$ /mL, mortality increased to 35% indicating that too few or too many inflammatory cells adversely affected the post-MI wound healing response.

Better biomarkers are needed to improve diagnosis, guide molecular target therapy, and monitor activity and therapeutic response in post-MI patients. An ideal biomarker has the following characteristics: high specificity, sensitivity, accessibility, speed, and cost-effectiveness [11]. Recent advances in genomic and proteomic approaches have increased the number of diagnostic marker candidates [12]. The Mississippi Center for Heart Research developed the Mouse Heart Attack Research Tool (mHART) as a means to consolidate results into an easily

<sup>☆</sup> This article is part of a Special Issue entitled: Genetic and epigenetic regulation of aging and longevity edited by Jun Ren & Megan Yingmei Zhang.

\* Corresponding author at: Department of Medicine, Division of Cardiology, Medical University of South Carolina, 30 Courtenay Drive, Charleston, SC 29425, USA.

E-mail address: [deleonky@musc.edu](mailto:deleonky@musc.edu) (K.Y. DeLeon-Pennell).

searchable format to facilitate broad use of big data analysis [13]. Because LV dilation is a strong predictor of post-MI survival [14], the goal of this study was to identify biomarkers that linked to the post-MI LV dilation phenotype. We hypothesized that using the mHART database would allow us to isolate the molecular and cellular LV dilation phenotype.

## 2. Materials and methods

### 2.1. Analysis of the mHART 1.0 database

The mHART database consists of data collected from projects published since 2007 for male and female mice ranging from 3 to 36 months of age. Data from the mHART database were collected from a single site lab with multiple investigators [13]. To limit inter-investigator variability, all experiments were collected under standard operating procedures that underwent periodical review by all lab members to prevent deviations in protocol. All data included in the mHART database underwent at least two quality control assessments, one initial at the time of collection and one at the time of inclusion in the database. The article describing the development of the database included a preliminary example of dilation responses. Here, we expand this original observation to identify molecular and cellular indicators that reflect LV dilation status.

#### 2.1.1. Sample selection

The database was accessed on April 15, 2017. Of 2095 mice downloaded, 759 were C57BL/6J post-MI mice. Of the 759 mice, 51 (31 males and 20 females) had serial echocardiography at day 0 (baseline) and at days 1 and 7 after MI and were between 3 and 9 months of age. Of the 51 mice, 39 (24 males and 15 females) had plasma measurements and 16 (8 males and 8 females) had immunohistochemistry measurements at day 7 post-MI. A 1.6 fold change in end diastolic dimension (EDD) was used as a cut-off point to distinguish groups, as this was the median value. Infarct size was determined by 1% 2,3,5-triphenyltetrazolium chloride staining and calculated as the percentage of infarct area to total LV area. Data from the male cohort were used to define the phenotype, and data from the females were used as the validation cohort. MI surgeries, echocardiography, and immunohistochemistry staining were performed according to established guidelines [15–17]. Echocardiography measurements were taken from the parasternal long axis B-mode and short axis M-mode views. To determine extent of LV remodeling, the 3D spherical index was calculated by dividing end diastolic volume by the volume of a sphere using the diameter from the major end-diastolic LV long axis.

#### 2.1.2. Data variables

In addition to echocardiography, plasma proteomics, immunohistochemistry, and gene array variables from the database were included. For plasma proteomic profiling, blood was collected from the common carotid artery in heparin. Proteinase inhibitor cocktail (1 × Complete; Roche, Indianapolis, IN) was added to the plasma, which was snap frozen at stored at  $-80^{\circ}\text{C}$  until use. Samples (100  $\mu\text{L}$ ) were sent to Myriad RBM (Austin, TX) for multi-analyte proteomic profiling of 56 analytes, of which 34 had detectable levels [18,19]. For immunohistochemistry, the LV middle section was fixed in 10% zinc formalin (Fisher Scientific), paraffin-embedded, and sectioned [18,19]. Heat mediated antigen retrieval (Target retrieval solution, Dako) was performed to expose antigen epitopes, followed by incubation in rabbit blocking serum (Vector Laboratories, Marion, IA). Tissue was incubated in a primary antibody specific for macrophages (Mac-3, Cedarlane, CL8943AP; 1:100) or neutrophils (PMNs; anti-neutrophil mouse monoclonal, Cedarlane, CL8993AP; 1:100) at  $4^{\circ}\text{C}$  overnight. Sections were incubated with the respective secondary antibodies and positive staining was visualized by HistoMark Black (KPL 54-75-00) and eosin was used as a counterstain. For gene array, RNA was extracted from LV

infarct tissue using PureLink RNA Mini Kit (Invitrogen, 12183-018A). RNA concentrations were determined using the NanoDrop ND-1000 Spectrophotometer (Thermo Scientific). Equal RNA (10 ng) was reversed transcribed using the High Capacity RNA-to-cDNA Kit (Life Technologies 4837406). Real Time RT<sup>2</sup>-PCR gene array for inflammatory cytokines and receptors (Qiagen PAMM-011A) and extracellular matrix (ECM; Qiagen PAMM-013A) was performed to quantify mRNA levels in the LV infarct. Values were normalized to *hprt1*, the only one of five housekeeping genes evaluated that did not change with MI [20].

### 2.2. RNA sequencing in isolated infarct macrophages

RNA extraction from macrophages for sequencing were pooled from  $n = 81$  hearts to obtain 4 biological replicates for each day post-MI [21]. LV macrophages were isolated from the infarct region by immunomagnetic separation as described previously [21–23]. Excised LV tissue was minced and digested by collagenase II (Worthington) and DNase solution in Hanks buffered saline solution. After digestion, a single cell suspension was generated by filtering through a 30  $\mu\text{m}$  pre-separation column followed by incubation at  $4^{\circ}\text{C}$  with an anti-Ly6G-biotin antibody (Miltenyi Biotech #130-092-332) to remove neutrophils. Cells were then incubated in an anti-CD11b-biotin antibody (Miltenyi #130-049-601) followed by anti-biotin microbeads (Miltenyi #130-092-332) for 10 min. Post-MI macrophages ( $\text{CD11b}^{+}\text{Ly6G}^{-}$ ;  $1.5 \times 10^6$  cells/well) were plated in 6-well culture dishes for 2 h in RPMI 1640 medium supplemented with 0.1% FBS and 10% antibiotics. After incubation, non-adherent cells were washed off and the remaining adherent cells were used for transcriptomics analysis by RNA-sequencing.

Whole transcriptome analysis was performed as described previously [23,24]. RNA was extracted using the Pure Link RNA Mini Kit (Ambion) according to manufacturer instructions and assessed for quality control parameters of minimum concentration and size range. cDNA libraries were developed using the TruSeq Total Stranded RNA with RiboZero Kit (Ambion), Set-A, quantified with the Qubit System (Invitrogen), and assessed for quality and size with the Experion DNA 1K Chip (Bio-Rad). The libraries were sequenced using the NextSeq 500 High Output Kit (300 cycles, paired end 100 bp) on the Illumina NextSeq 500 platform. Sequenced reads were assessed for quality using the Illumina BaseSpace Onsite Computing Platform, and Fastq sequence files were used to align reads to the reference genome USCS-GRCh38/mm10. The full dataset has been published in a study that mapped out the macrophage profile over the post-MI time course [21].

### 2.3. Bioinformatics and statistical analyses

Post-MI LV EDD values were normalized to baseline no MI values, and the median was calculated to separate groups. GraphPad Prism 7 was used for statistical analysis. For two group comparisons, unpaired *t*-test was used for normally distributed data; otherwise, the nonparametric Wilcoxon rank sum test was used. Partial least squares discriminant analysis (PLS-DA) was used for assessment of distribution. Plasma analytes from the extreme group were normalized to values for the moderate group to generate comparison datasets, which were inputted into the pathway analysis program within the Metaboanalyst 4.0 package ([www.metaboanalyst.ca/](http://www.metaboanalyst.ca/)) [25,26]. The Z-score for pathway analysis was based on the mean and standard deviation of the extreme samples and compared to the moderate group. Areas under ROC curves (AUC) were calculated using GraphPad Prism 7 statistics software. The appropriate threshold values for sensitivity and specificity were determined at the point at which the maximum sensitivity + specificity – 1 was obtained. A value of  $p < 0.05$  was considered statistically significant.

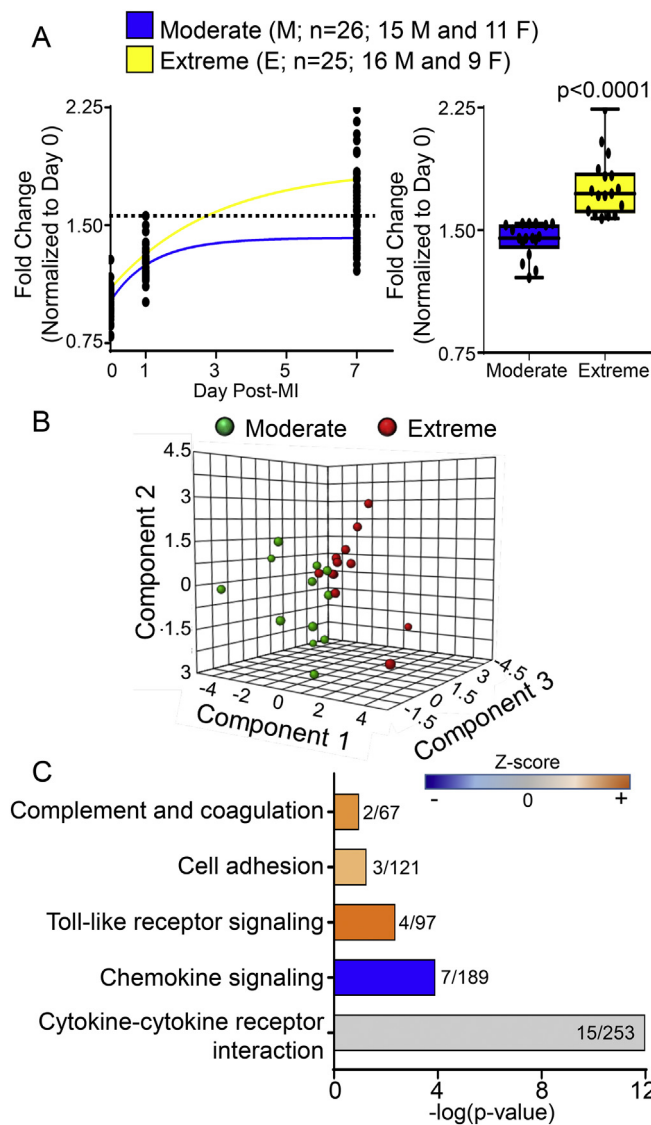


**Fig. 1.** Two distinct dilation response groups were identified. (A) Using mHART, a median change in end diastolic dimension (EDD) of 1.6 fold, mice were classified into moderate and extreme groups. (B) Partial least squares discriminant analysis (PLS-DA) of 34 plasma analytes from mHART revealed separate clustering of the two groups. (C) By pathway analysis, chemokine signaling was downregulated (blue) and toll-like receptor, cell adhesion, and complement and coagulation were upregulated (orange) in the extreme group compared to the moderate group. No differences were observed in cytokine-cytokine receptor interaction (gray). Z-score was calculated based on the mean and standard deviation of extreme compared to moderate.

### 3. Results

#### 3.1. Clustering of EDD identified two distinct LV dilation response groups

Serial measurements of EDD combined from both sexes distinguished LV dilation into moderate ( $< 1.6$  fold change) and extreme ( $> 1.6$  fold change) responses (Fig. 1A). The average fold change at day 7 for the moderate group was  $1.42 \pm 0.01$  and for the extreme group was  $1.79 \pm 0.01$  ( $p < 0.001$ ). End systolic dimension, infarct wall thickness, end diastolic and systolic volumes, fractional shortening, and ejection fraction were significantly different between dilation groups ( $p < 0.05$  for all), indicating the change in EDD was a good marker of remodeling status. The differences in the two groups were not due to sex or other physiological attributes, including heart rate or infarct size

**Table 1**

Physiological measurements of moderate and extreme groups at day 7 post-myocardial infarction shows physiological differences were not due to age, sex, or infarct size.

	Moderate	Extreme	p value
Age, months	$5.8 \pm 0.1$	$5.4 \pm 0.1$	0.32
Sex, males/females (% females)	15/11 (42%)	16/9 (36%)	0.78
Infarct size, % infarct	$50 \pm 1$	$54 \pm 1$	0.16
Body weight, g	$24 \pm 1$	$23 \pm 1$	0.76
Heart rate, bpm	$485 \pm 1$	$477 \pm 1$	0.58
Left ventricle mass, mg	$98 \pm 1$	$101 \pm 1$	0.69
Right ventricle mass, mg	$25 \pm 1$	$21 \pm 1$	0.07
Wall thickness, systole mm	$0.62 \pm 0.01$	$0.48 \pm 0.02$	0.002
End diastolic dimension, mm	$5.20 \pm 0.02$	$6.28 \pm 0.03$	$< 0.001$
End systolic dimension, mm	$4.88 \pm 0.03$	$6.06 \pm 0.03$	$< 0.001$
Fractional shortening, %	$6 \pm 1$	$4 \pm 1$	0.002
End diastolic volume, $\mu\text{L}$	$111 \pm 1$	$165 \pm 2$	$< 0.001$
End systolic volume, $\mu\text{L}$	$96 \pm 1$	$151 \pm 2$	$< 0.001$
Ejection fraction, %	$15 \pm 1$	$9 \pm 1$	$< 0.001$

(Table 1).

As a first pass test, male plasma samples ( $n = 12$  moderate and 12 extreme) were analyzed to identify biomarkers that tracked with dilation. Sparse classification of the partial least squares discriminant analysis (sPLS-DA) of the 34 plasma analytes indicated distinct separation between groups (Fig. 1B). By pathway analysis, differentially expressed analytes highly associated with regulation of inflammation (Fig. 1C). Chemokine signaling was significantly downregulated while toll-like receptor, cell adhesion, and complement and coagulation were significantly upregulated in the extreme group compared to the moderate group. No differences were identified in the cytokine-cytokine receptor interaction between the extreme and moderate groups.

#### 3.2. Reduced macrophage inflammatory protein (MIP)-1 $\gamma$ , granulocyte chemotactic protein (GCP-2), and lymphotactin were strong indicators of dilation status

As published previously, Euclidean's hierarchical unsupervised clustering of the plasma analytes within the male cohort, the two groups clustered separately based on plasma analyte expression profiles. Averages of the plasma profiles are shown in Fig. 2A. By unpaired *t*-test, plasma MIP-1 $\gamma$ , lymphotactin, and GCP-2 were the only proteins lower in the extreme group compared to the moderate group (Fig. 2B–D). This is consistent with a decrease in the chemokine signaling shown in Fig. 1C. Of note, none of the plasma analytes were increased in the extreme group.

By ROC analysis, MIP-1 $\gamma$  had an AUC of 0.81 and was a strong indicator of moderate LV dilation in males (Fig. 3A). GCP-2 and lymphotactin both had AUC values of at least 0.7 (Fig. 3B–C). Myeloperoxidase (MPO) is a biomarker shown to independently predict the risk of major adverse cardiac events in the 1-month and 6-month periods after an MI [9,27]. At day 7 post-MI, MPO had an AUC of 0.63 ( $p = 0.27$ ; Fig. 3D). By unpaired *t*-test, MPO ( $p = 0.12$ ) was not different between groups. Neutrophil-mediated inflammation at day 7 is almost fully resolved, which explains why MPO was not a strong indicator of day 7 LV dilation.

As a second pass validation, plasma MIP-1 $\gamma$ , GCP-2, and lymphotactin were analyzed in females ( $n = 6$  moderate and 9 extreme) using the 1.6 fold change cut-off value. In females, MIP-1 $\gamma$  was significantly lower in the extreme group, similar to what was observed in the males (Fig. 4A). MIP-1 $\gamma$  negatively correlated with EDD values (Fig. 4B) and ROC analysis showed an AUC of 0.85 (Fig. 4C;  $p = 0.02$ ) supporting the hypothesis that MIP-1 $\gamma$  is a strong indicator of beneficial cardiac wound healing. While plasma GCP-2 concentration in females was not significantly different by *t*-test ( $p = 0.09$ ), by ROC analysis, GCP-2 was a strong predictor of LV dilation state (AUC = 0.83,  $p = 0.04$ ; Fig. 4D).

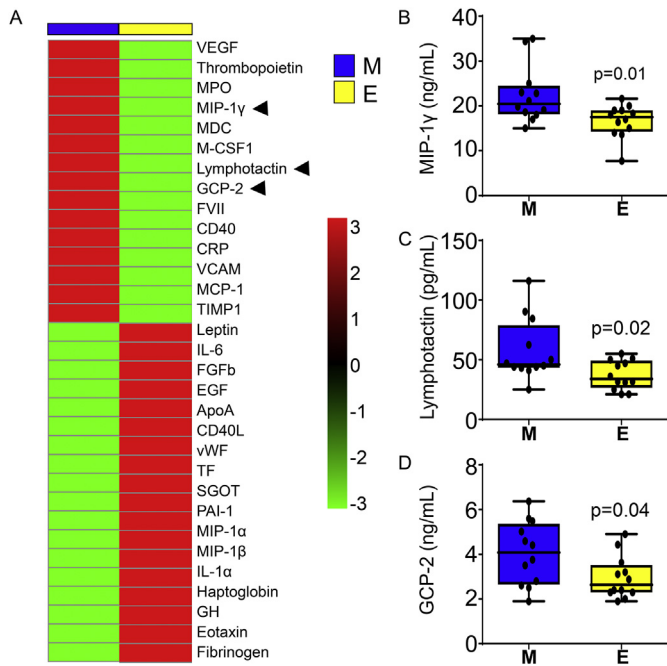


**Fig. 2.** Analysis of plasma proteins identified potential indicators that correlate with dilation outcome. (A) Heat map of the top 15 differentially expressed plasma analytes (mHART plasma proteomic dataset) showed strong clustering of groups based on protein profiles; 3 were significantly downregulated in the extreme group compared to the moderate group (◄). (B) Macrophage inflammatory protein (MIP)1 $\gamma$ , (C) lymphotactin, and (D) granulocyte chemotactic protein (GCP)2 were significantly lower in the extreme dilation group. n = 12 male mice/group.

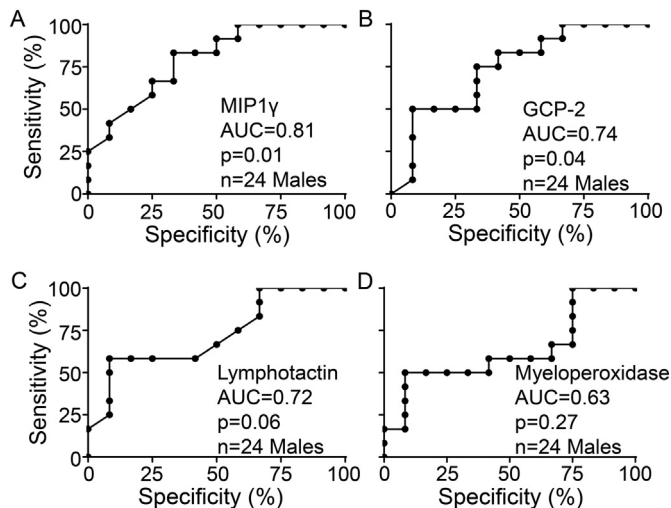


**Fig. 3.** MIP1 $\gamma$ , GCP-2, and lymphotactin were strong indicators of moderate LV dilation in males. By ROC analysis (A) high circulating MIP-1 $\gamma$  at day 7 post-MI was a strong indicator of moderate LV dilation. (B) Granulocyte chemotactic protein (GCP)2, and (C) lymphotactin were also strong indicators of moderate LV dilation. (D) Myeloperoxidase (MPO) was not a strong indicator of day 7 post-MI LV dilation. Plasma proteomic data collected from males within mHART was used for analysis. n = 12 male mice/group.

Lymphotactin (p = 0.42) was not significantly different by t-test and had an AUC of < 0.7 in the female validation set, similar to what was shown in the male cohort.

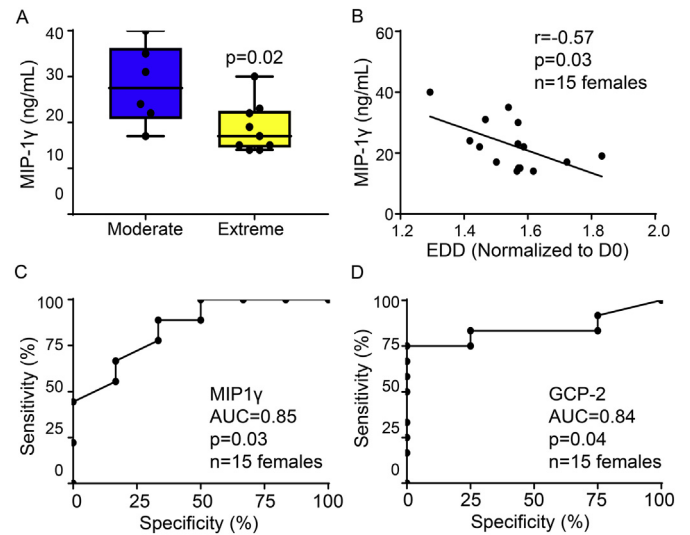


**Fig. 4.** Validation using a separate MI cohort of females also identifies MIP1 $\gamma$  and GCP-2 as indicators of moderate LV dilation. (A) Using a separate cohort of female day 7 post-MI mice (n = 6 moderate; n = 9 extreme), MIP-1 $\gamma$  was significantly reduced in the extreme dilation group. (B) MIP-1 $\gamma$  negatively correlated with end diastolic dimension (EDD) and ROC analysis indicated (C) MIP1 $\gamma$  and (D) GCP-2 were strong indicator of LV dilation. Plasma proteomic data collected from females within mHART was used for analysis.

### 3.3. Macrophage numbers negatively correlated with LV dilation status

To determine if LV dilation status was a reflection of leukocyte numbers, we evaluated neutrophil and macrophage numbers in the day 7 post-MI LV infarct (Fig. 5). No difference was observed in neutrophil numbers between the dilation groups (p = 0.46). Of note, macrophage numbers were lower in the extreme group compared to the moderate group, in line with the downregulation of chemokine signaling observed in the plasma. By ROC analysis, neutrophil numbers had an AUC of 0.57 (p = 0.64) and macrophage numbers had an AUC of 0.83 (p = 0.03), implicating macrophages as being a key reflection of dilation phenotype. The reduced macrophage numbers in the extreme group highlight the importance of the macrophage in the repair process [19,28,29].

Of 184 inflammatory and fibrotic genes evaluated in the LV infarct, three (complement C5, laminin 1, and Ccr8) were significantly elevated in the extreme group (Fig. 6A). This is consistent with the increase in complement and coagulation and cell adhesion pathways (Fig. 1C). No genes were significantly downregulated. Gene expression of MIP-1 $\gamma$  (p = 0.18) in the LV infarct was not significantly different between groups, indicating that the differences observed in the plasma were post-transcriptional. Lymphotactin and GCP-2 were not measured in the gene array. Out of the three genes significantly different between LV groups, Ccr8 was the only one that positively correlated with EDD (r = 0.51; p = 0.01) and negatively correlated with macrophage numbers (r = -0.66; p = 0.04), indicating Ccr8 gene was an indicator of extreme dilation (Fig. 6B-C). C5 (r = 0.21; p = 0.53) and laminin 1 (r = 0.52; p = 0.10) did not correlate to EDD values. By ROC analysis, Ccr8 had an AUC of 0.75 (p = 0.04; Fig. 6D). Ccr8 and MIP-1 $\gamma$  did not associate with each other (r = 0.20; p = 0.64), indicating these markers likely work independently.

### 3.4. Macrophage highly expressed MIP-1 $\gamma$ and correlated with spherical index

To determine the cellular source of the biomarkers identified, we isolated macrophages from the infarct at days 0, 1, 3, and 7 post-MI and assessed their genomic profile [21]. Of the three plasma markers

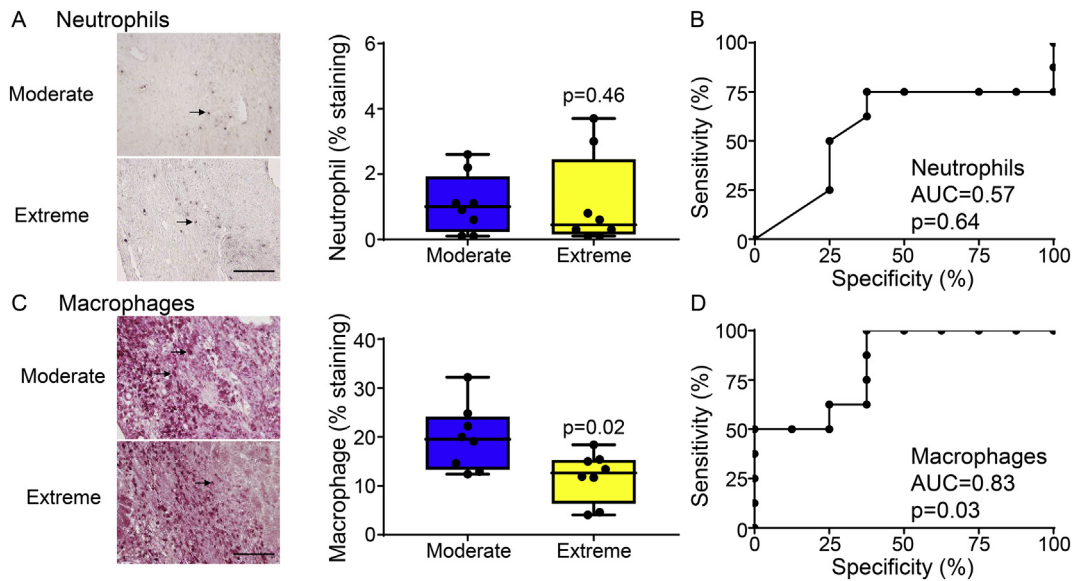


**Fig. 5.** Extreme dilator group had fewer macrophages without differences in neutrophil numbers. (A) No difference in neutrophil numbers at day 7 post-MI between groups (arrows depict positive staining). (B) ROC analysis indicated neutrophil numbers did not reflect LV dilation status. (C) Macrophage numbers were significantly lower in the extreme group compared to the moderate group (arrows depict positive staining) and (D) ROC analysis indicated macrophage numbers reflected LV dilation state. Immunohistochemistry data collected from mHART was used for analysis. Scale bar, 60 μM.

identified using mHART, only MIP-1γ was found to be expressed by post-MI macrophages (Fig. 7A). Macrophage expression of MIP-1γ peaked at post-MI day 1 and by day 7 was lower than post-MI day 0 macrophages.

To dissect if macrophage expression of these biomarkers was responsible for the dilation status, we calculated the spherical index that reflects LV eccentric remodeling in post-MI patients [30]. Spherical index negatively correlated with macrophage numbers, indicating that macrophages prevented LV dilation (Fig. 7B). Mice with fewer macrophages had increased spherical index signifying a larger, rounder LV. Interestingly, MIP-1γ had a non-linear relationship with macrophage cell numbers, indicating too much or too little MIP-1γ may be a negative regulator of macrophage recruitment (Fig. 7C). This is in line with what we observed with our extreme phenotype that had lower levels of macrophages and decreased Ccl9 levels. Our data indicates that macrophage secretion of Ccl9 is partially responsible for LV dilation status.

**3.5. Composite multi-marker strategy improves indication of LV dilation state**

To test the feasibility of using a multi-marker strategy to improve the indication of LV dilation status, we assessed 5 biomarkers: plasma MIP-1γ, lymphotactin, and GCP-2, and LV infarct Ccr8 and macrophage numbers (Fig. 8). Using a five panel test improved determination of LV dilation state (AUC = 0.92; p < 0.001). The addition of laminin 1 or complement C5 decreased the AUC to below 0.7, consistent with the lack of individual association. Despite not being a strong predictor alone, lymphotactin when added to MIP-1γ, GCP-2, Ccr8, and macrophage numbers increased the AUC from 0.85 for the 4 indicators to 0.92.

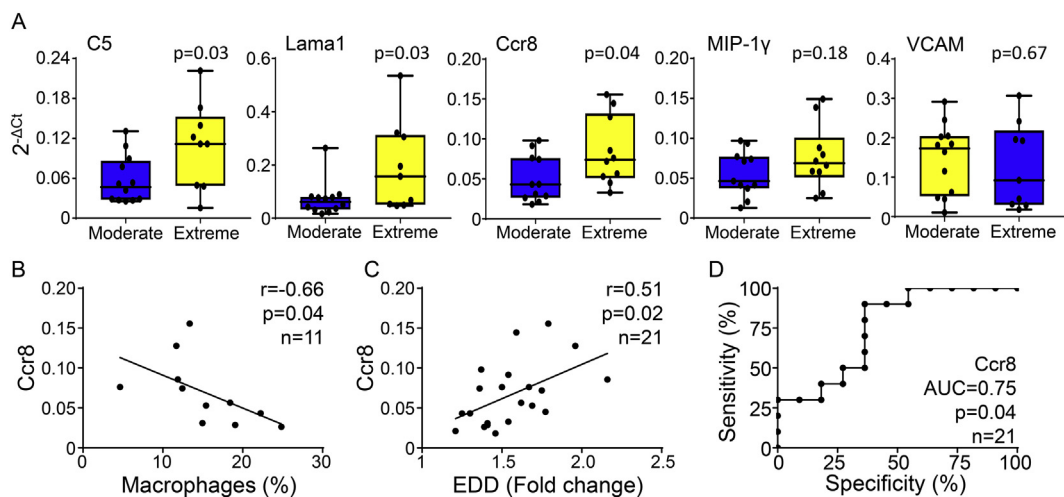
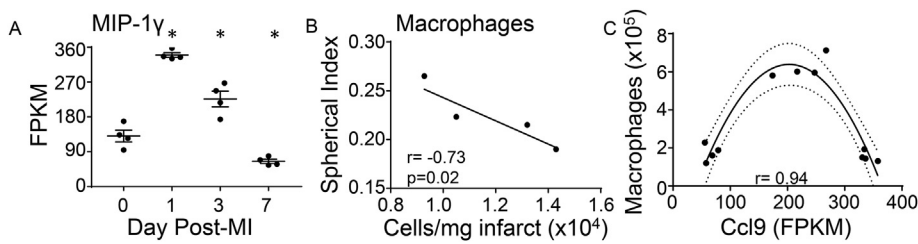


**Fig. 6.** Elevated Ccr8 gene expression in the day 7 infarct predicts extreme dilation. (A) Assessment of 184 genes collected from the mHART database indicated C5, laminin a1 (Lama1), and Ccr8 were significantly higher in the day 7 infarct of extreme dilators compared to the moderate group. MIP-1γ gene expression in the infarct was not significantly different between groups indicating plasma differences were post-transcriptional. (B) Ccr8 negatively correlated with macrophages in the infarct area and (C) positively correlated with EDD. (D) ROC analysis substantiated Ccr8 as an indicator of LV dilation.



rophage numbers indicating too much or too little MIP-1 $\gamma$  may be a negative regulator of macrophage recruitment. Data was generated from a separate cohort of mice [21].  $n = 81$  mice total with  $n = 4$  pooled biological replicates/day post-MI. \* $p < 0.05$  vs day 0. FPKM = fragments per kilobase million.

A

Biomarker	Extreme compared to moderate	AUC	p value
MIP1 $\gamma$ (plasma)	↓	0.81	0.014
Lymphotactin (plasma)	↓	0.72	0.065
GCP-2 (plasma)	↓	0.74	0.044
Ccr8 (LVI gene)	↑	0.75	0.043
LVI Macrophage number	↓	0.83	0.027

B

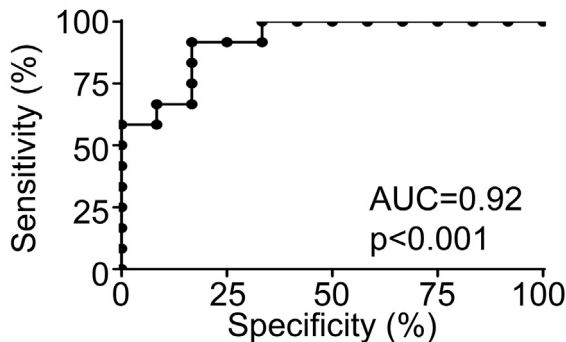


Fig. 8. Multi-marker strategy with key independent biomarkers improves indication of LV dilation status. (A) Single marker ROC analysis of MIP-1 $\gamma$ , lymphotactin, GCP-2, Ccr8, and macrophage numbers using males and females ( $n = 18$  moderate;  $n = 21$  extreme). (B) Using a five panel test improved determination of LV dilation state. All data was collected from the mHART database.

#### 4. Discussion

The goal of this study was to use the mHART database to identify an extreme post-MI LV dilation phenotype. Elevated plasma MIP-1 $\gamma$ , GCP-2, and lymphotactin along with decreased LV infarct expression of Ccr8 and increased macrophage numbers, were identified as strong indicators of the moderate LV dilation phenotype. Our results indicate that a failure to mount a sufficient macrophage response linked with adverse remodeling after MI more than an overabundant response. Using the mHART database, we were able to identify a composite multimarker panel that included MIP-1 $\gamma$ , GCP-2, and lymphotactin from the plasma, as well as Ccr8 and macrophage numbers from the LV infarct, as being a strong indicator panel for LV dilation status.

This is the first report that has assigned a positive role for MIP-1 $\gamma$  in post-MI wound healing. MIP-1 $\gamma$ /Ccl9 is a chemotactic protein secreted by neutrophils and macrophages that regulates the wound healing response in multiple disease processes, including cutaneous wound healing [31–34]. MIP-1 $\gamma$  inhibition reduces neutrophil and macrophage

infiltration, collagen deposition, and improves pulmonary function in a mouse model of chronic graft-versus-host disease [33]. MIP-1 $\gamma$  has been shown to correlate with the extent of atherosclerotic lesions [35]. While not previously evaluated in the MI setting, a similar inhibition phenotype would be detrimental for MI remodeling. In addition, in a model of colon cancer, MIP-1 $\gamma$  promotes recruitment of the matrix metalloproteinase-expressing stromal cells [32], consistent with a positive role in necrotic tissue removal.

Overexpression of GCP-2 has been linked to improved LV remodeling by increasing pro-angiogenic and anti-apoptotic gene expression within the infarct [36]. Less is known about the role of lymphotactin (Xcl1) during the cardiac remodeling processes, in part due to conflicting results. In a rat model of cardiac allograft, lymphotactin was linked to accelerated allograft rejection [37]. In contrast, lymphotactin expression was not associated with rejection in cardiac allograft recipients [38]. Ccr8 is primarily expressed by regulatory T-cells and is known to regulate monocyte chemotaxis [39,40]. In left ventricular assist device patients, decreased Ccr8 expression was found to correlate with increased 1 year mortality [41]; however, its post-MI role has not been extensively studied.

Multiple studies have shown negative [42–44] and positive [45–47] correlations between monocyte and macrophage numbers and MI LV remodeling. Macrophages regulate a number of wound healing events, including removal of cell debris, development of the infarct scar, and angiogenesis [2,21]. In a recent publication, we demonstrated that at day 1 post-MI, the macrophage exhibits a pro-inflammatory phenotype and by day 7 post-MI, macrophages exhibit a reparative phenotype that indirectly contributes to ECM formation through release of paracrine factors and directly secretes ECM proteins (collagen and periostin) [21]. Decreased day 7 reparative macrophages would exacerbate LV remodeling resulting in the extreme dilator phenotype.

White blood cell count within 24 h of admission for an MI (inflammatory phase) is a strong and independent predictor of in-hospital and 30-day mortality as well as in-hospital clinical events [7]. Our data indicated that during the later maturation phase of wound healing, neutrophil numbers are not strong predictors for adverse remodeling. Neutrophils likely have an indicator role early during days 1–3 after MI during the phase that neutrophils are the prominent cell type. Macrophages become the primary cell at around post-MI day 5 making these cells ideal for predicting LV changes during the proliferative and maturation phase of cardiac wound healing.

A strength of using the multimarker panel is that despite having overlap, each of the biomarkers regulate separate pathways of the LV remodeling process. For example, MIP-1 $\gamma$  regulates macrophage recruitment, while GCP-2 is a pro-angiogenic protein secreted by macrophages and lymphotactin and Ccr8 are markers of T-cell mediated inflammation [36,39,48–50]. Having biomarkers that incorporate multiple aspects of MI remodeling can improve specificity and sensitivity because they are not inter-dependent [51,52]. Another strength is that the plasma results alone provided a strong composite indicator, which improves ease of use and cost-effectiveness. Future evaluations to determine if these markers have translational relevance in clinical cohorts are warranted.

In summary, this is the first report to detail LV dilation phenotypes after MI in mice and identify plasma proteins and LV infarct inflammatory cells and genes that explain the differences in dilation.

### Transparency document

The [Transparency document](#) associated with this article can be found, in online version.

### Acknowledgments

We acknowledge funding from the American Heart Association [15SDG22930009], from the National Institutes of Health [GM104357, GM114833, GM115428, HL051971, HL075360, HL105324, and HL129823], and from the Biomedical Laboratory Research and Development Service of the VA Office of Research and Development [5I01BX000505 and IK2BX003922]. The content is solely the responsibility of the authors and does not necessarily represent the official views of the American Heart Association, the National Institutes of Health, or the Veterans Administration. All authors have reviewed and approved the article. All authors have read the journal authorship agreement and policy on disclosure of potential conflicts of interest and have nothing to disclose.

### Disclosures

None.

### References

- [1] K.Y. DeLeon, A. Yabluchanskiy, M.D. Winniford, R.A. Lange, R.J. Chilton, M.L. Lindsey, Modifying matrix remodeling to prevent heart failure, in: R. Li, R.D. Weisel (Eds.), *Cardiac Regeneration and Repair, Pathology and Therapies*, vol. 1, Woodhead, 2013.
- [2] M.L. Lindsey, J.J. Saucerman, K.Y. DeLeon-Pennell, Knowledge gaps to understanding cardiac macrophage polarization following myocardial infarction, *Biochim. Biophys. Acta* 1862 (2016) 2288–2292.
- [3] K.Y. DeLeon-Pennell, C.A. Meschiaro, M. Jung, M.L. Lindsey, Matrix metalloproteinases in myocardial infarction and heart failure, *Prog. Mol. Biol. Transl. Sci.* 147 (2017) 75–100.
- [4] M.L. Lindsey, Regulating macrophage infiltration to alter wound healing following myocardial infarction, *Cardiovasc. Res.* (2018), <https://doi.org/10.1093/cvr/cvy146>.
- [5] A.J. Mouton, O.J. Rivera Gonzalez, M.L. Lindsey, Myocardial infarction remodeling that progresses to heart failure: a signaling misunderstanding, *Am. J. Physiol. Heart Circ. Physiol.* 315 (2018) H71–H79.
- [6] V. Kain, F. Liu, V. Kozlovskaya, K.A. Ingle, S. Bolisetty, A. Agarwal, S. Khedkar, S.D. Prabhu, E. Kharlampieva, G.V. Halade, Resolution agonist 15-epi-Lipoxin A4 programs early activation of resolving phase in post-myocardial infarction healing, *Sci. Rep.* 7 (2017) 9999.
- [7] H.V. Barron, S.D. Harr, M.J. Radford, Y. Wang, H.M. Krumholz, The association between white blood cell count and acute myocardial infarction mortality in patients  $\geq 65$  years of age: findings from the cooperative cardiovascular project, *J. Am. Coll. Cardiol.* 38 (2001) 1654–1661.
- [8] A. Albadri, K. Lai, J. Wei, S. Landes, P.K. Mehta, Q. Li, D. Johnson, S.E. Reis, S.F. Kelsey, V. Bittner, G. Sopko, L.J. Shaw, C.J. Pepine, C.N. Bairey Merz, Inflammatory biomarkers as predictors of heart failure in women without obstructive coronary artery disease: a report from the NHLBI-sponsored Women's Ischemia Syndrome Evaluation (WISE), *PLoS One* 12 (2017) e0177684.
- [9] M.C. Meuwese, E.S. Stroes, S.L. Hazen, J.N. van Miert, J.A. Kuivenhoven, R.G. Schaap, N.J. Wareham, R. Luben, J.J. Kastelein, K.T. Khaw, S.M. Boekholdt, Serum myeloperoxidase levels are associated with the future risk of coronary artery disease in apparently healthy individuals: the EPIC-Norfolk Prospective Population Study, *J. Am. Coll. Cardiol.* 50 (2007) 159–165.
- [10] M. Grzybowski, R.D. Welch, L. Parsons, C.E. Ndumele, E. Chen, R. Zalenski, H.V. Barron, The association between white blood cell count and acute myocardial infarction in-hospital mortality: findings from the National Registry of Myocardial Infarction, *Acad. Emerg. Med.* 11 (2004) 1049–1060.
- [11] H. Zhou, S.M. Hewitt, P.S. Yuen, R.A. Star, Acute kidney injury biomarkers - needs, present status, and future promise, *Nephrol. Self-Assess. Program* 5 (2006) 63–71.
- [12] D.M. Good, V. Thongboonkerd, J. Novak, J.L. Bascands, J.P. Schanstra, J.J. Coon, A. Dominiczak, H. Mischak, Body fluid proteomics for biomarker discovery: lessons from the past hold the key to success in the future, *J. Proteome Res.* 6 (2007) 4549–4555.
- [13] K.Y. DeLeon-Pennell, R.P. Iyer, Y. Ma, A. Yabluchanskiy, R. Zamilpa, Y.A. Chiao, P. Cannon, C. Cates, E.R. Flynn, G.V. Halade, L.E. de Castro Bras, M.L. Lindsey, The mouse heart attack research tool (mHART) 1.0 database, *Am. J. Physiol. Heart Circ. Physiol.* 113 (2018) 26 (in press).
- [14] P. Gaudron, I. Kugler, K. Hu, W. Bauer, C. Eilles, G. Ertl, Time course of cardiac structural, functional and electrical changes in asymptomatic patients after myocardial infarction: their inter-relation and prognostic impact, *J. Am. Coll. Cardiol.* 38 (2001) 33–40.
- [15] H.L. Brooks, M.L. Lindsey, Guidelines for authors and reviewers on antibody use in physiology studies, *Am. J. Physiol. Heart Circ. Physiol.* 314 (2018) H724–H732.
- [16] M.L. Lindsey, Z. Kassiri, J.A.I. Virag, L.E. de Castro Bras, M. Scherrer-Crosbie, Guidelines for measuring cardiac physiology in mice, *Am. J. Physiol. Heart Circ. Physiol.* 314 (2018) H733–H752.
- [17] M.L. Lindsey, R. Bolli, J.M. Canty, X.J. Du, N.G. Frangogiannis, S. Frantz, R.G. Gourdie, J.W. Holmes, S.P. Jones, R. Kloner, D.J. Lefer, R. Liao, E. Murphy, P. Ping, K. Przyklenk, F.A. Recchia, L. Schwartz Longacre, C.M. Ripplinger, J.E. Van Eyk, G. Heusch, Guidelines for experimental models of myocardial ischemia and infarction, *Am. J. Physiol. Heart Circ. Physiol.* 314 (2018) H812–H838.
- [18] K.Y. DeLeon-Pennell, L.E. de Castro Bras, R.P. Iyer, D.R. Bratton, Y.F. Jin, C.M. Ripplinger, M.L. Lindsey, *P. gingivalis* lipopolysaccharide intensifies inflammation post-myocardial infarction through matrix metalloproteinase-9, *J. Mol. Cell. Cardiol.* 76C (2014) 218–226.
- [19] K.Y. DeLeon-Pennell, R.P. Iyer, O.K. Ero, C.A. Cates, E.R. Flynn, P.L. Cannon, M. Jung, D. Shannon, M.R. Garrett, W. Buchanan, M.E. Hall, Y. Ma, M.L. Lindsey, Periodontal-induced chronic inflammation triggers macrophage secretion of Cell12 to inhibit fibroblast-mediated cardiac wound healing, *JCI Insight* 2 (2017) e94207.
- [20] M.L. Lindsey, R.P. Iyer, R. Zamilpa, A. Yabluchanskiy, K.Y. DeLeon-Pennell, M.E. Hall, A. Kaplan, F.A. Zouein, D. Bratton, E.R. Flynn, P.L. Cannon, Y. Tian, Y.F. Jin, R.A. Lange, D. Tokmina-Roszyk, G.B. Fields, L.E. de Castro Bras, A novel collagen matricryptin reduces left ventricular dilation post-myocardial infarction by promoting scar formation and angiogenesis, *J. Am. Coll. Cardiol.* 66 (2015) 1364–1374.
- [21] A.J. Mouton, K.Y. DeLeon-Pennell, O.J. Rivera Gonzalez, E.R. Flynn, T.C. Freeman, J.J. Saucerman, M.R. Garrett, Y. Ma, R. Harmancey, M.L. Lindsey, Mapping macrophage polarization over the myocardial infarction time continuum, *Basic Res. Cardiol.* 113 (2018) 26.
- [22] K.Y. DeLeon-Pennell, A.J. Mouton, O.K. Ero, Y. Ma, R. Padmanabhan Iyer, E.R. Flynn, I. Espinoza, S.K. Musani, R.S. Vasan, M.E. Hall, E.R. Fox, M.L. Lindsey, LXR/RXR signaling and neutrophil phenotype following myocardial infarction classify sex differences in remodeling, *Basic Res Cardiol.* 113 (2018) 40.
- [23] M. Jung, Y. Ma, R.P. Iyer, K.Y. DeLeon-Pennell, A. Yabluchanskiy, M.R. Garrett, M.L. Lindsey, IL-10 improves cardiac remodeling after myocardial infarction by stimulating M2 macrophage polarization and fibroblast activation, *Basic Res. Cardiol.* 112 (2017) 33.
- [24] C.A. Meschiaro, M. Jung, R.P. Iyer, A. Yabluchanskiy, H. Toba, M.R. Garrett, M.L. Lindsey, Macrophage overexpression of matrix metalloproteinase-9 in aged mice improves diastolic physiology and cardiac wound healing after myocardial infarction, *Am. J. Physiol. Heart Circ. Physiol.* 314 (2018) H224–H235.
- [25] T.H. Vu, J.M. Shipley, G. Bergers, J.E. Berger, J.A. Helms, D. Hanahan, S.D. Shapiro, R.M. Senior, Z. Werb, MMP-9/gelatinase B is a key regulator of growth plate angiogenesis and apoptosis of hypertrophic chondrocytes, *Cell* 93 (1998) 411–422.
- [26] J. Xia, I.V. Sinelnikov, B. Han, D.S. Wishart, *MetaboAnalyst 3.0*—making metabolomics more meaningful, *Nucleic Acids Res.* 43 (2015) W251–W257.
- [27] M.L. Brennan, M.S. Penn, F. Van Lente, V. Nambi, M.H. Shishehbor, R.J. Aviles, M. Goormastic, M.L. Pepoy, E.S. McErlane, E.J. Topol, S.E. Nissen, S.L. Hazen, Prognostic value of myeloperoxidase in patients with chest pain, *N. Engl. J. Med.* 349 (2003) 1595–1604.
- [28] M. Nahrendorf, F.K. Swirski, Monocyte and macrophage heterogeneity in the heart, *Circ. Res.* 112 (2013) 1624–1633.
- [29] M. Hulsmans, F. Sam, M. Nahrendorf, Monocyte and macrophage contributions to cardiac remodeling, *J. Mol. Cell. Cardiol.* 93 (2016) 149–155.
- [30] D. Zeng, H. Chen, C.L. Jiang, J. Wu, Usefulness of three-dimensional spherical index to assess different types of left ventricular remodeling: a meta-analysis, *Medicine (Baltimore)* 96 (2017) e7968.
- [31] V. Kain, K.A. Ingle, R.A. Colas, J. Dalli, S.D. Prabhu, C.N. Serhan, M. Joshi, G.V. Halade, Resolvin D1 activates the inflammation resolving response at splenic and ventricular site following myocardial infarction leading to improved ventricular function, *J. Mol. Cell. Cardiol.* 84 (2015) 24–35.
- [32] T. Kitamura, M.M. Taketo, Keeping out the bad guys: gateway to cellular target therapy, *Cancer Res.* 67 (2007) 10099–10102.
- [33] J. Du, R. Flynn, K. Paz, H.G. Ren, Y. Ogata, Q. Zhang, P.R. Gafken, B.E. Storer, N.H. Roy, J.K. Burkhardt, W. Mathews, J. Tolar, S.J. Lee, B.R. Blazar, S. Paczesny, Murine chronic graft-versus-host disease proteome profiling discovers CCL15 as a novel biomarker in patients, *Blood* 131 (2018) 1743–1754.
- [34] S. Kagawa, A. Matsuo, Y. Yagi, K. Ikematsu, R. Tsuda, I. Nakasono, The time-course analysis of gene expression during wound healing in mouse skin, *Legal Med.* 11 (2009) 70–75.
- [35] R. Tabibiazar, R.A. Wagner, A. Deng, P.S. Tsao, T. Quertermous, Proteomic profiles of serum inflammatory markers accurately predict atherosclerosis in mice, *Physiol. Genomics* 25 (2006) 194–202.
- [36] S.W. Kim, D.W. Lee, L.H. Yu, H.Z. Zhang, C.E. Kim, J.M. Kim, T.H. Park, K.S. Cha, S.Y. Seo, M.S. Roh, K.C. Lee, J.S. Jung, M.H. Kim, Mesenchymal stem cells over-expressing GCP-2 improve heart function through enhanced angiogenic properties in a myocardial infarction model, *Cardiovasc. Res.* 95 (2012) 495–506.
- [37] D.N. Streblov, C. Kreklywich, Q. Yin, V.T. De La Melena, C.L. Corless, P.A. Smith, C. Brakebill, J.W. Cook, C. Vink, C.A. Bruggeman, J.A. Nelson, S.L. Orloff, Cytomegalovirus-mediated upregulation of chemokine expression correlates with the acceleration of chronic rejection in rat heart transplants, *J. Virol.* 77 (2003)

- 2182–2194.
- [38] M. Melter, A. Exeni, M.E. Reinders, J.C. Fang, G. McMahon, P. Ganz, W.W. Hancock, D.M. Briscoe, Expression of the chemokine receptor CXCR3 and its ligand IP-10 during human cardiac allograft rejection, *Circulation* 104 (2001) 2558–2564.
- [39] C. Qu, E.W. Edwards, F. Tacke, V. Angeli, J. Llodra, G. Sanchez-Schmitz, A. Garin, N.S. Haque, W. Peters, N. van Rooijen, C. Sanchez-Torres, J. Bromberg, I.F. Charo, S. Jung, S.A. Lira, G.J. Randolph, Role of CCR8 and other chemokine pathways in the migration of monocyte-derived dendritic cells to lymph nodes, *J. Exp. Med.* 200 (2004) 1231–1241.
- [40] Y. Barsheshet, G. Wildbaum, E. Levy, A. Vitenshtein, C. Akinseye, J. Griggs, S.A. Lira, N. Karin, CCR8(+)FOXP3(+) Treg cells as master drivers of immune regulation, *Proc. Natl. Acad. Sci. U. S. A.* 114 (2017) 6086–6091.
- [41] A. Nayak, C. Neill, R.L. Kormos, L. Lagazzi, I. Halder, C. McTiernan, J. Larsen, A. Inashvili, J. Teuteberg, T.N. Bachman, K. Hanley-Yanez, D.M. McNamara, M.A. Simon, Chemokine receptor patterns and right heart failure in mechanical circulatory support, *J. Heart Lung Transplant.* 36 (2017) 657–665.
- [42] K. Kaikita, T. Hayasaki, T. Okuma, W.A. Kuziel, H. Ogawa, M. Takeya, Targeted deletion of CC chemokine receptor 2 attenuates left ventricular remodeling after experimental myocardial infarction, *Am. J. Pathol.* 165 (2004) 439–447.
- [43] S. Hayashidani, H. Tsutsui, T. Shiomi, M. Ikeuchi, H. Matsusaka, N. Suematsu, J. Wen, K. Egashira, A. Takeshita, Anti-monocyte chemoattractant protein-1 gene therapy attenuates left ventricular remodeling and failure after experimental myocardial infarction, *Circulation* 108 (2003) 2134–2140.
- [44] Y. Maekawa, T. Anzai, T. Yoshikawa, Y. Sugano, K. Mahara, T. Kohno, T. Takahashi, S. Ogawa, Effect of granulocyte-macrophage colony-stimulating factor inducer on left ventricular remodeling after acute myocardial infarction, *J. Am. Coll. Cardiol.* 44 (2004) 1510–1520.
- [45] J. Leor, L. Rozen, A. Zulloff-Shani, M.S. Feinberg, Y. Amsalem, I.M. Barbash, E. Kachel, R. Holbova, Y. Mardor, D. Daniels, A. Ocherashvilli, A. Orenstein, D. Danon, Ex vivo activated human macrophages improve healing, remodeling, and function of the infarcted heart, *Circulation* 114 (2006) 194–100.
- [46] H. Morimoto, M. Takahashi, A. Izawa, H. Ise, M. Hongo, P.E. Kolattukudy, U. Ikeda, Cardiac overexpression of monocyte chemoattractant protein-1 in transgenic mice prevents cardiac dysfunction and remodeling after myocardial infarction, *Circ. Res.* 99 (2006) 891–899.
- [47] F.K. Swirski, M. Nahrendorf, M. Etzrodt, M. Wildgruber, V. Cortez-Retamozo, P. Panizzi, J.L. Figueiredo, R.H. Kohler, A. Chudnovskiy, P. Waterman, E. Aikawa, T.R. Mempel, P. Libby, R. Weissleder, M.J. Pittet, Identification of splenic reservoir monocytes and their deployment to inflammatory sites, *Science* 325 (2009) 612–616.
- [48] M. Yang, P.R. Odgren, Molecular cloning and characterization of rat CCL9 (MIP-1gamma), the ortholog of mouse CCL9, *Cytokine* 31 (2005) 94–102.
- [49] A.D. Cristillo, M.J. Macri, B.E. Bierer, Differential chemokine expression profiles in human peripheral blood T lymphocytes: dependence on T-cell coreceptor and calcineurin signaling, *Blood* 101 (2003) 216–225.
- [50] S. Struyf, M. Gouwy, C. Dillen, P. Proost, G. Opendakker, J. Van Damme, Chemokines synergize in the recruitment of circulating neutrophils into inflamed tissue, *Eur. J. Immunol.* 35 (2005) 1583–1591.
- [51] T.J. Wang, P. Gona, M.G. Larson, G.H. Tofler, D. Levy, C. Newton-Cheh, P.F. Jacques, N. Rifai, J. Selhub, S.J. Robins, E.J. Benjamin, R.B. D'Agostino, R.S. Vasani, Multiple biomarkers for the prediction of first major cardiovascular events and death, *N. Engl. J. Med.* 355 (2006) 2631–2639.
- [52] S. Kathiresan, P. Gona, M.G. Larson, J.A. Vita, G.F. Mitchell, G.H. Tofler, D. Levy, C. Newton-Cheh, T.J. Wang, E.J. Benjamin, R.S. Vasani, Cross-sectional relations of multiple biomarkers from distinct biological pathways to brachial artery endothelial function, *Circulation* 113 (2006) 938–945.